Electronic Supplementary Material (ESI) for Physical Chemistry Chemical Physics.

Supplementary Information for Thermal Conductivity of Fivefold Twinned Silicon-Germanium Heteronanowires

Ziyue Zhou[1], Jincheng Zeng[1], Zixuan Song[1], Yanwen Lin[1], Qiao Shi[1], Yongchao Hao[1], Yuequn Fu[2,*], Zhisen Zhang[1,*] and Jianyang Wu[1,3,*]

[1]*Department of Physics, Research Institute for Biomimetics and Soft Matter, Jiujiang Research Institute and Fujian Provincial Key Laboratory for Soft Functional Materials Research, Xiamen University, Xiamen 361005, PR China*

[2]*PoreLab, the Njord Centre, Department of Physics, University of Oslo, Oslo 0316, Norway*

[3]*NTNU Nanomechanical Lab, Norwegian University of Science and Technology (NTNU), Trondheim 7491, Norway*

[*]Corresponding Emails: yuequn.fu@fys.uio.no, zhangzs@xmu.edu.cn and jianyang@xmu.edu.cn

S1 Methods for thermal conductivity (κ) calculations

S1.1 The HNEMD method

On the basis of the non-canonical linear-response theory, the HNEMD method was first proposed by Evans et al.[1] in terms of two-body potentials. Recently, it was extended to general many-body potentials[2] and integrated into the GPUMD package. In this method, to drive investigated system out of equilibrium, an external force is added to atom *i* after equilibration with the following expression as

$$\vec{F}_i^{ext} = E_i \vec{F}_e + \sum_{j \neq i} \left(\frac{\partial U_j}{\partial \vec{r}_{ji}} \otimes \vec{r}_{ij} \right) \cdot \vec{F}_e, \tag{S1}$$

where E_i is the total energy of particle *i* and U_i is the potential energy. The position difference $\vec{r}_{ij}$ is defined as $\vec{r}_{ij} \equiv \vec{r}_j - \vec{r}_i$. $\vec{F}_e$ is a vector that represents the driving force. As a result, the "hotter" atoms in the systems are pushed along the heat transport direction (*x* direction), while the "cooler" atoms in the systems are pulled in the opposite direction. However, investigated systems maintain the global temperature near the target temperature (300 K) using a Nosé-Hoover thermostat[3,4]. Then, an ensemble average steady-state nonequilibrium heat current $\langle J(t) \rangle_{\text{ne}}$ that is proportional to the magnitude of the parameter $\vec{F}_e$ is generated. Finally, the κ along heat transport direction is calculated as follows

$$\kappa(t) = \frac{1}{t} \int_0^t \frac{\langle J(t) \rangle_{\text{ne}}}{TVF_{\text{e}}} dt, \tag{S2}$$

where t, V and T is the production time, the volume and the temperature of investigated system, respectively. In the HNEMD method, the driving force parameter $\vec{F}_e$ is required to be chosen carefully to ensure a large data signal-to-noise ratio within the linear response of the system[2]. There is a rule of thumb stating that, as $\vec{F}_e \lambda_{\text{max}} \lesssim 1$ in which λ_{max} is the maximum phonon mean free path (MFP), the linear response is guaranteed.

S1.2 The NEMD method

The NEMD method is an inhomogeneous method to calculate the κ of a material in finite size because a heat source and a sink are required. In NEMD calculations, a Langevin thermostat with a coupling time of 0.1 ps[5, 6] is adopted to generate the temperatures of the heat source and sink in this work. The κ of Si-NWs in the axial transport direction is determined as follows[5]

$$\kappa(L) = \frac{dE/dt}{S\Delta T/L}, \tag{S3}$$

where S and L are the cross-sectional area and the effective axial length of NWs, respectively. The dE/dt and ΔT are the average energy exchange rate and the temperature difference between the thermostats, respectively.

S1.3 Spectral heat current decomposition

To provide the physical insights underlying the MD results, the phonon properties of Si-NWs are calculated. The phonon frequency-dependent MFP and the length-dependent $\kappa(L)$ are determined by the spectral heat current (SHC) decomposition method[2, 7-9]. In this method, the spectral conductance $G(\omega)$ in the ballistic regime and the spectral conductivity $\kappa(\omega)$ in the diffusive regime are calculated by NEMD and HNEMD simulations, respectively. As a result, the spectral phonon MFP is determined as follows

$$\lambda(\omega) = \frac{\kappa(\omega)}{G(\omega)}. \tag{S4}$$

Then, $\kappa(L)$ is calculated as follows[2]

$$\kappa(L) = \int_0^\infty \frac{d\omega}{2\pi} \kappa(\omega, L), \tag{S5}$$

Where

$$\frac{1}{\kappa(\omega, L)} = \frac{1}{\kappa(\omega)}\left(1 + \frac{\lambda(\omega)}{L}\right). \tag{S6}$$

S2 Results of Thermal Conductivity Calculations

The results of HNEMD calculations for typical five-fold twinned silicon nanowires (5FT-Si-NWs) and bulk Si are shown in Fig. S1. The complete data are listed in Table SI. M is the number of independent runs, while N indicates the number of atoms the system contains. κ_{ave} (in units of W m^{-1} K^{-1}) is the average thermal conductivity and its standard error is κ_{err}. The unit of $\vec{F}_e$ is μm^{-1}, and the unit of area S is nm^2. Due to the significant difference in thermal conductivity of different structures calculated by HNEMD, $\vec{F}_e$ varies and the number of independent runs also varies.

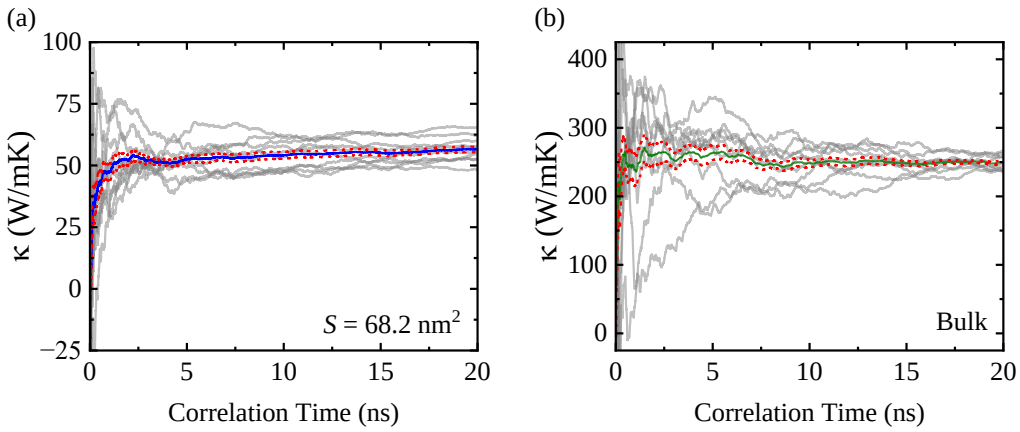

Fig. S1 (a-b) Partial thermal conductivity results computed by HNEMD. The thick solid line represents the average of the thin solid line (multiple independent runs; each run has a different initial velocity). The red dotted line indicates the statistical error range.

TABLE S1 Relevant data from the HNEMD simulations.

S	Structure	N	HNEMD			
			M	F_e	κ_{ave}	κ_{err}
/	Bulk	3456	15	0.1	249.67	2.43
1.2	Si	3500	10	0.03	148.59	12.11
	Ge				52.34	5.85
	20%				84.99	6.77

	40%-A				75.89	7.36
	40%-S				93.22	6.94
	60%-A				60.83	8.06
	60%-S				75.28	6.15
	80%				62.05	5.81
4.6	Si	8500	10	0.03	79.46	5.32
	Ge				34.13	3.71
	20%				43.40	3.09
	40%-A				35.94	2.39
	40%-S				49.13	3.78
	60%-A				27.07	1.71
	60%-S				38.49	3.72
	80%				31.85	3.07
10.2	Si	15500	10	0.03	64.18	2.92
	Ge				25.53	1.14
	20%				34.37	1.69
	40%-A				28.76	0.86
	40%-S				36.51	1.28
	60%-A				23.32	1.22
	60%-S				30.36	1.56
	80%				26.87	1.04
16.7	Si	24500	10	0.03	52.93	1.65
	Ge				24.36	1.83
	20%				27.86	1.13
	40%-A				23.61	0.76
	40%-S				22.14	1.23
	60%-A				22.06	0.69
	60%-S				20.98	0.72
	80%				21.58	0.73
26.3	Si	35500	10	0.03	55.86	2.18
	Ge				24.36	1.05
	20%				27.83	0.98

	40%-A				24.22	0.74
	40%-S				23.27	0.46
	60%-A				23.17	0.83
	60%-S				21.49	0.45
	80%				22.15	0.68
37.4	Si	48500	10	0.03	56.16	1.27
	Ge				24.52	1.06
	20%				30.78	0.57
	40%-A				27.09	0.56
	40%-S				24.16	0.41
	60%-A				24.41	0.53
	60%-S				22.74	0.52
	80%				22.72	0.71
51.3	Si	63500	10	0.03	56.53	0.92
	Ge				24.97	1.01
	20%				32.21	0.52
	40%-A				27.72	0.42
	40%-S				25.27	0.35
	60%-A				24.57	0.29
	60%-S				23.77	0.32
	80%				23.09	0.79
68.2	Si	80500	10	0.03	56.58	1.11
	Ge				25.01	0.51
	20%				32.92	0.26
	40%-A				28.67	0.36
	40%-S				26.64	0.57
	60%-A				25.21	0.77
	60%-S				24.11	0.34
	80%				23.64	0.47

S3 Size Effect of HNEMD

Here, 5FT-Si-NW with area of 10.2 nm^2 is used to calibrate the size effect of HNEMD. It is clear

from Fig. S2. that HNEMD simulation can ignore the size effect when the length of 5FT-Si-NWs reaches 80 unit-cells (about 31.01 nm). The thermal conductivity reported in this paper corresponds to the system length of 100 unit-cells (about 38.77 nm).

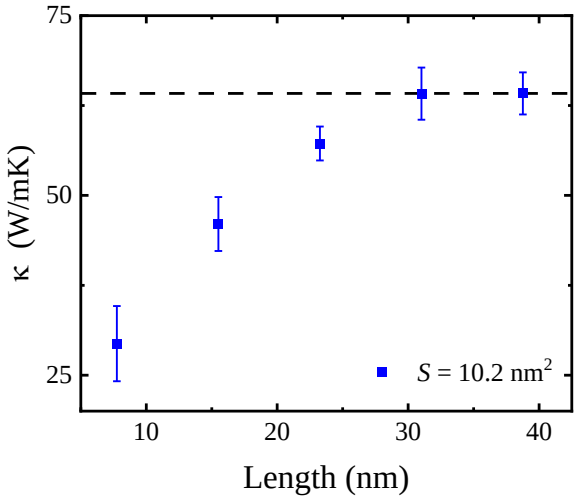

Fig. S2. Size effect of HNEMD method on κ of 5FT-Si-NWs with different length.

S4 The Static and Thermodynamic Stability

It is a popular method to use temperature and energy of a system as the criterion to determine the thermodynamic stability of a system. In addition, phonon dispersion is often used as a criterion to evaluate whether the system is statically stable. Here, thermodynamic and static criteria are used to determine the stability of the system. The results on phonon dispersion are given in the main text. The temperature and energy of the system as a function of time during the simulation is discussed in the most detailed model used in the main text, and the results are presented in Fig. S3. In Fig. S3, we can easily find that the temperature and energy will become thermodynamically stable when the *S* of 5FT-Si-NW reaches 1.2 nm^2. Therefore, all the systems used in this work are both statically and thermodynamically stable.

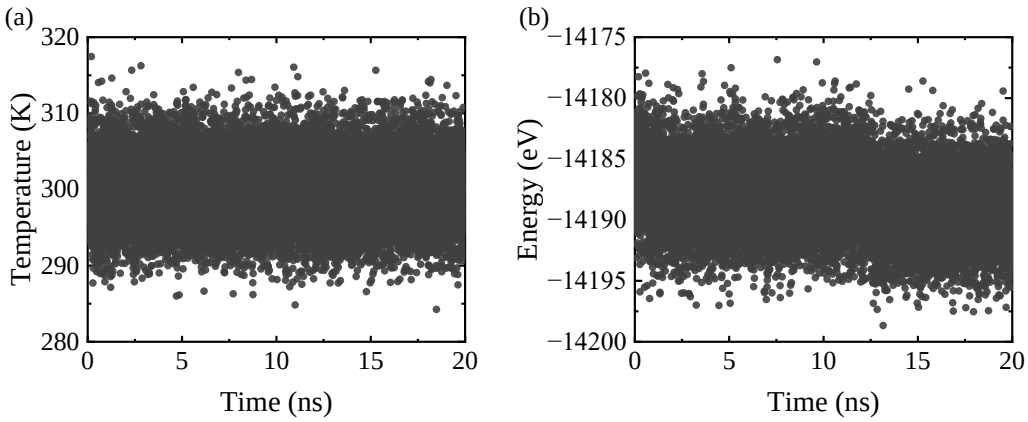

Fig. S3. The (a) temperature and (b) energy of 5FT-Si-NW with a *S* of 1.2 nm^2 using Tersoff potential.

S5 Phonon properties of 5FT-Si-NWs with different *S*

To further understand the phonon properties of 5FT-Si-NWs with different S, we conducted separate calculations for nanowires of varying sizes to analyze the phonon dispersion relations and three-phonon scattering.

The phonon dispersion relations of nanowires with different sizes were calculated, and it was observed that an overall downward shift of the optical branch occurs with an increase in *S*, as depicted in Fig. S4. This phenomenon explains the decrease in thermal conductivity as the area increases in extremely thin cases.

Additionally, we performed calculations for three-phonon scattering in 5FT-Si-NW models with different *S* values, and the corresponding results are presented in Fig. S5. It was found that as *S* decreases, the differences between the N-process and U-process become significantly larger, indicating an increase in thermal conductivity with decreasing *S*. This trend aligns with previous studies on the subject[10, 11].

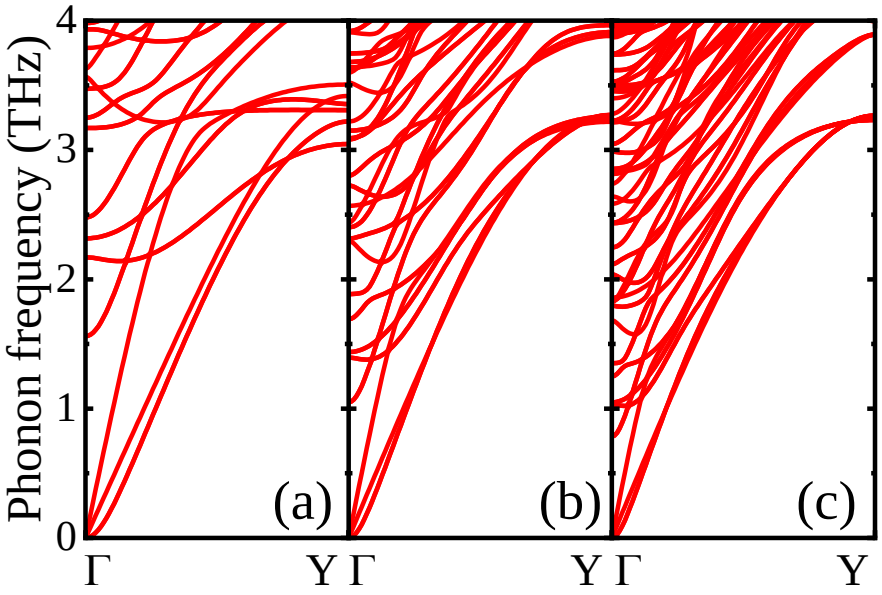

Fig. S4. Phonon dispersion curves of 5FT-Si-NWs with (a) S = 1.2 nm^2, (b) S = 4.6 nm^2 and (c) S = 10.2 nm^2, respectively, in which the phonon frequency is limited to be below 4 THz for highlighting the differences of acoustic and optics phonons.

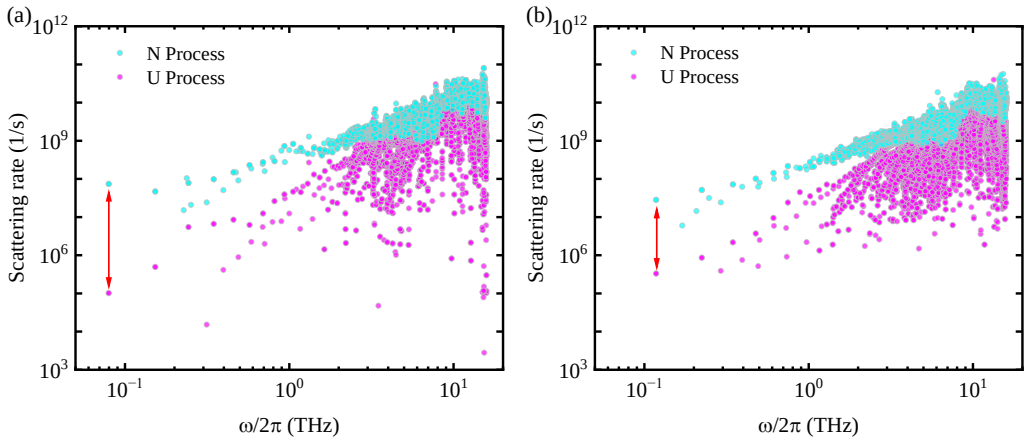

Fig. S5. The three-phonon scattering rates of 5FT-Si-NWs with (a) S = 1.2 nm^2 and (b) S = 4.6 nm^2 as a function of phonon frequency, including Normal (N) and Umklapp (U) processes. The red arrows indicate the differences in the magnitude of the scattering rate between the U and N processes.

S6 Phonon Properties of Bulk Silicon

In order to validate the validity of phonon dispersion and three-phonon scattering rates in

nanowires, we have conducted calculations on the phonon properties of bulk silicon in this study. The phonon dispersion of bulk silicon is presented in Figure S5(a), and our findings are in excellent agreement with those reported in reference[12].

For the bulk silicon analysis, a 3 × 3 × 3 supercell and a 30 × 30 × 30 q-point grid were employed to ensure accurate sampling of the first Brillouin zone and obtain reliable results for three-phonon scattering rates, as depicted in Figure S5(b). In bulk silicon, the difference between the N and U processes at low frequencies is within one order of magnitude, which is smaller compared to NWs. This observation aligns with the findings reported in reference[11].

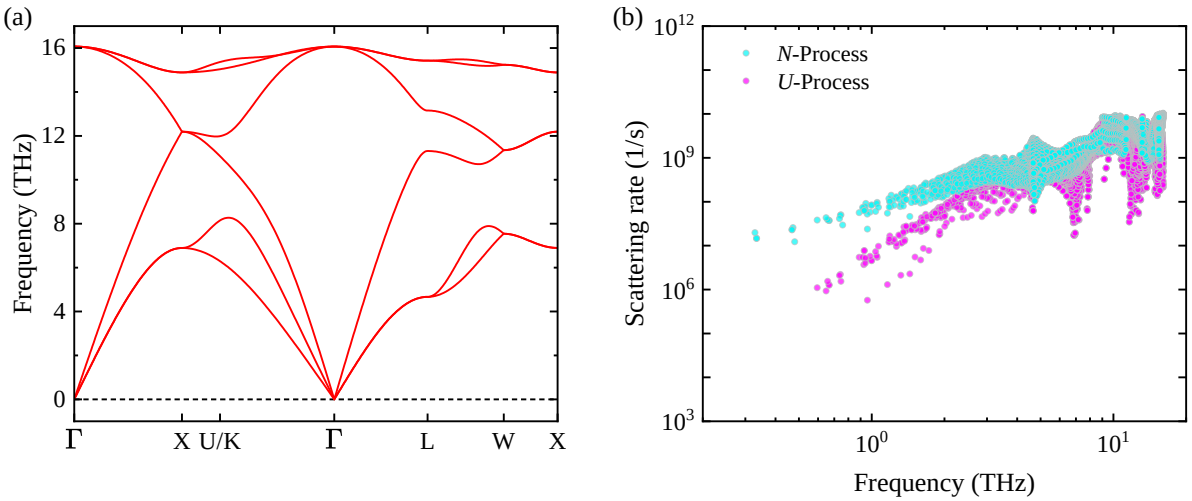

Figure S6. Phonon dispersion (a) and three-phonon scattering rates (b) of bulk silicon.

References

1. D. J. Evans, *Phys. Lett. A*, 1982, **91**, 457-460.
2. Z. Y. Fan, H. K. Dong, A. Harju and T. Ala-Nissila, *Phys. Rev. B*, 2019, **99**.
3. S. Nose, *J. Chem. Phys.*, 1984, **81**, 511-519.
4. W. G. Hoover, *Phys. Rev. A*, 1985, **31**, 1695-1697.
5. Z. Li, S. Xiong, C. Sievers, Y. Hu, Z. Fan, N. Wei, H. Bao, S. Chen, D. Donadio and T. Ala-Nissila, *J. Chem. Phys.*, 2019, **151**, 234105.
6. Y. Hu, T. Feng, X. Gu, Z. Fan, X. Wang, M. Lundstrom, S. S. Shrestha and H. Bao, *Phys. Rev. B*, 2020, **101**, 155308.
7. K. Sääskilahti, J. Oksanen, S. Volz and J. Tulkki, *Phys. Rev. B*, 2015, **91**, 115426.

8. Z. Fan, L. F. C. Pereira, P. Hirvonen, M. M. Ervasti, K. R. Elder, D. Donadio, T. Ala-Nissila and A. Harju, *Phys. Rev. B*, 2017, **95**, 144309.
9. A. J. Gabourie, Z. Fan, T. Ala-Nissila and E. Pop, *Phys. Rev. B*, 2021, **103**, 205421.
10. T. Liang, K. Xu, M. Han, Y. Yao, Z. Zhang, X. Zeng, J. Xu and J. Wu, *Mater. Today Phys.*, 2022, **25**, 100705.
11. Y. Zhou, X. Zhang and M. Hu, *Nano Lett.*, 2017, **17**, 1269-1276.
12. Z. Fan, Y. Wang, X. Gu, P. Qian, Y. Su and T. Ala-Nissila, *J. Phys.: Condens. Matter*, 2019, **32**, 135901.